Nuclear Inst. and Methods in Physics Research, A 1000 (2021) 165248

Contents lists available at ScienceDirect

Nuclear Inst. and Methods in Physics Research, A

journal homepage: www.elsevier.com/locate/nima

# Monitoring of the unattached fraction of radon progeny by the Kodak LR-115 Type 2, nuclear track detector

Jiri Kvasnicka [a,*], Vladimir Zdimal [b], Allan Seini [c]

[a] Radiation Detection Systems, Unit 10, 186 Pulteney Street, Adelaide 5000, Australia
[b] Institute of Chemical Process Fundamentals, Czech Academy of Sciences, Rozvojova 135, 16502 Prague 6, Czech Republic
[c] Energy Resources Australia (ERA), Ranger Mine, Arnhem Highway, Jabiru NT 0886, Australia

ARTICLE INFO

*Keywords:*
Nuclear track detector Kodak LR-115
$^{214}$Po alpha radiation detection
Radon progeny
Unattached fraction of radon progeny

ABSTRACT

The experimental Unattached Radon Progeny Fraction Monitor (URPFM) was developed for the parallel monitoring of all radon progeny and the fraction of radon progeny in air that is attached onto aerosols. The optimum monitor arrangement includes two radon progeny sampling columns with each column incorporating a 0.8 μm membrane filter. The filter in the first sampling column collects all the ambient radon progeny that are measured by the Kodak LR-115 nuclear track detector. The second sampling column also includes a fine mesh that removes the unattached radon progeny from the sampled air and thus the track detector that is situated above the mesh measures the unattached radon progeny.

Three, five to thirteen-day long radon progeny monitoring periods were conducted inside a sealed room of a residential house and outdoors at an open cut uranium mine. The average unattached fraction of radon progeny was measured to be between 0.09 and 0.14 for the residential house, and between 0.08 and 0.10 for the open cut uranium mine.

## 1. Introduction

### 1.1. Review of radon progeny dosimetry

The effective dose (ED) due to the potential alpha energy exposure (PAEE) of the radon progeny is calculated by the use of a conversion factor of 1.4 mSv per mJ h m$^{-3}$ that was derived for adults from epidemiological studies of underground miners and from residential studies [1].

More recently the International Commission on Radiological Protection (ICRP) adopted the dosimetric approach to derive the ED to the PAEE of radon progeny conversion factors [2]. This new approach considers aerosol parameters of individual radon progeny and namely the fraction of radon progeny that are not attached onto airborne aerosols i.e. unattached fraction of radon progeny ($f_p$). The factor $f_p$ is the ratio of the potential alpha energy concentration that is attributed to the unattached radon progeny compared to the total one. The inhalation of the unattached fraction of radon progeny yields a much higher ED than the inhalation of radon progeny that are attached to aerosols. For example, the ED per unit radon progeny PAEE was derived as 3.1 mSv per mJ h m$^{-3}$ and 5.6 mSv per mJ h m$^{-3}$ for mines and indoor workplaces respectively [2]. These conversion factors took into account a $f_p$ = 0.08 for indoor workplaces and 0.01 for mines with forced ventilation. The radon equilibrium factors (F) of 0.4 and 0.2 were considered for indoor workplaces and for mines respectively.

It is, therefore, anticipated that the ICRP dosimetric approach and new conversion factors would be used when legislated. Such approach would have to include studies based on the monitoring of the unattached fraction of radon progeny in the workplace.

### 1.2. Assessment of the personal radon progeny effective dose

The personal ED due to the exposure to radon progeny in a workplace is based on the long-term monitoring of the PAEC of radon progeny:

$$ED = PAEC \times ET \times CF \quad (1)$$

where :

(a) PAEC (mJ m$^{-3}$) is the measured long-term average potential alpha energy concentration;
(b) ET(h) is the exposure time: and
(c) CF = 1.4 (mSv per mJ h m$^{-3}$) is the currently used ED to the PAEE conversion factor [1].

The ICRP effective dose calculation methodology recommended to use a CF of 3.1 mSv per mJ h m$^{-3}$ for mines and 5.6 mSv per mJ h

* Corresponding author.
*E-mail addresses:* rdsjk@ozemail.com.au (J. Kvasnicka), Zdimal@icpf.cos.ca (V. Zdimal), Allan.Seini@rio.tinto.com (A. Seini).

https://doi.org/10.1016/j.nima.2021.165248
Received 17 June 2020; Received in revised form 8 March 2021; Accepted 10 March 2021
Available online 17 March 2021
0168-9002/

$m^{-3}$ for indoor workplaces [2]. The unattached fraction of 0.08 was considered for indoor workplaces and 0.01 for underground mines with forced ventilation.

In case the unattached fraction was measured the ED calculation formula (1) uses:

$CF = 24\ f_p + 3.9\ (1 - f_p)$ for indoor workplaces; and

$CF = 24\ f_p + 2.9\ (1 - f_p)$ for mines. It is important to use long-term average $f_p$ values in the ED assessment.

Uranium mines and other workplaces include a variety of work environments where the levels of radon and radon progeny and aerosol concentrations in air vary significantly. It is, therefore, important to have a suitable unattached fraction monitoring method that can provide longer-term average unattached fraction values in critical work environments.

### 1.3. Unattached fraction monitoring

The separation of the unattached fraction of radon progeny from those attached to aerosols and the monitoring of the separated unattached fraction is a "complex" experimental task. A practical and accurate enough method for the separation and the monitoring of the unattached and attached fraction of radon progeny needs to be developed so that the ICRP dosimetric approach could be adopted.

The measurements of radon progeny activity size distribution cover the range from about 0.5 to 300 nm in diameter and were carried out with multi-stage diffusion batteries [3–6].

Considering the substantial differences in the diffusion properties of the unattached radon fraction aerosols below 5 nm and of the attached fraction of aerosols it is possible to use a single wire screen on which the unattached fraction would be deposited while the attached fraction would pass through [5,7–9]. A diffusion model is then used to calculate the penetration of the unattached fraction through the single screen.

## 2. Experimental part

### 2.1. Monitoring instrumentation

The main aim of any unattached/attached fraction monitoring method should be to obtain long-term average figures of $f_p$ that could be used with the long-term average PAEE of radon progeny to estimate the personal ED.

In order to carry out the monitoring under several experimental arrangements the unattached radon progeny fraction monitor (URPFM) was constructed. The URPFM consists of a precisely regulated air sampling pump (the flow rate was set at 0.5 L $min^{-1}$). The air sampler draws air through two air sampling columns (Fig. 1). The individually calibrated flow rate monitoring gauges are in-line between the column and the air sampler so that the flow rate through each column can be individually checked. The constant air flow rate through each column was set to 0.25 L $min^{-1}$ and was measured by the "bubble" airflow monitor. The flow rate through the second column containing the mesh was found to be approximately 1.7% lower than the flow rate through the column without the mesh. This change was due to the minute resistance to the airflow caused by the fine mesh.

The first column included the $\Phi$25 mm × 0.8 μm Millipore membrane filter with the Kodak-LR115 Type 2, nuclear track detectors situated above the filter. The second column included the same filter as above and either one or two Kodak-LR115 Type 2, nuclear track detectors for the detection of alpha particles emitted by radon progeny collected on the filter and/or on the mesh.

**Table 1**
Radon decay series.

| Nuclide | Half-life | Radiation | Alpha Energy (MeV) | Intensity (%) |
|---|---|---|---|---|
| $^{222}$Rn (Radon) | 3.82 d | $\alpha$ | 5.48 | 100 |
| $^{218}$Po | 3.05 m | $\alpha$ | 6.00 | 100 |
| $^{214}$Pb | 26.8 m | $\beta$ | | |
| $^{214}$Bi | 19.9 m | $\beta$ | | |
| $^{214}$Po | 164 μs | $\alpha$ | 7.69 | 100 |
| $^{210}$Pb | 22 y | $\beta$ | | |
| $^{210}$Bi | 5.0 d | $\beta$ | | |
| $^{210}$Po | 138 d | $\alpha$ | 5.30 | 100 |
| $^{206}$Pb (Stable) | | | | |

### 2.2. Detection of $^{214}$Po alpha particles by Kodak LR-115

The Kodak-LR115, nuclear track detector has been used for the detection of alpha radiation and for the monitoring of long-term average radon activity concentrations in air and the PAEC of radon progeny [10,11]. The detection efficiency of the nuclear track detector depends on the residual energy of alpha particles at the detector surface impact point, the impact angle of the alpha particle and on the etching conditions [12,13]. The above parameters can be optimized so only the tracks caused by alpha particles within a narrow energy range can be detected.

The nuclear track detector was overlaid by aluminized mylar film that had a surface weight of 3 mg $cm^{-2}$ and was situated 20 mm above the filter and/or the mesh (Fig. 1). After exposure the detector was etched for 100 min in a 10% NaOH solution which was maintained at a temperature of 60 °C.

The described experimental and the well controlled etching conditions were chosen to ensure that the constant layer of the detector sensitive layer is removed by etching and thus only alpha particles of $^{214}$Po that were emitted from the filter and/or the mesh could be detected as "through etched" alpha tracks. Alpha particles of radon and thoron progeny that emit alpha radiation with the energy below 7.7 MeV are either completely attenuated by a column of air and the mylar film or their residual energy at the detector surface is too low so they produce only dark tracks that were not etched through i.e. were not counted. The 8.8 MeV alpha radiation of 212Po (the thoron progeny) has too high residual energy to produce through etched bright tracks (the tracks of the higher energy than 7.7 MeV are observed under a microscope as very small minute tracks or they produce no tracks at all).

The detection of alpha radiation of $^{214}$Po as described above has one fundamental advantage: whilst only alpha particles of $^{214}$Po are measured, the nuclear track detector implicitly detects all radon progeny including beta radiation emitting radon progeny that are detected indirectly (Table 1). All radon progeny collected on the filter and/or the mesh during sampling transform by the decay to $^{214}$Po that emits alpha radiation. Therefore, the nuclear track detector represents the "true" integral monitor of radon progeny in air during log-term sampling.

## 3. Monitoring results

**Filter/filter experiment**

The first column of the UFRDM included a $\Phi$25 mm x 0.8 μm Millipore filter with the nuclear track detector situated 20 mm above the filter. The second column was the same as the first one but had the mesh between the air inlet of the column and the track detector that was situated 20 mm above the filter. The nuclear track detector in the first column detected the alpha radiation of $^{214}$Po emitted by radon progeny on the filter that were both attached and unattached onto aerosols. The nuclear track detector in the second column detected the alpha radiation of $^{214}$Po emitted by radon progeny on the filter that were only attached onto aerosols.


**Fig. 1.** The unattached radon progeny fraction monitor (URPFM)

The UFRDM was used to monitor radon progeny during three, five to seven-day sampling periods. The indoor monitoring was conducted inside of a closed room with sealed doors and windows of a residential ground level house. Outdoor monitoring was conducted at the Energy Resources of Australia (ERA) Ranger Uranium mine in the Northern Territory of Australia, where the monitor was situated approximately 1.8 m above the ground between two uranium ore stockpiles.

The monitoring results for the closed room were summarized in Table 2 and for the open cut uranium mine in Table 3.

The nuclear track values in Tables 2 and 3 were obtained by counting tracks on the same area of the nuclear track, which was between 22.8 $mm^2$ and 51.2 $mm^2$ (tracks on two nuclear track detectors from the same exposure were counted on the same surface area). One relative standard deviation of counted track figures was between 2.7% and 5.1%.

**Filter/mesh experiment**

The monitoring experiments were carried out inside of the same closed room as above and lasted between eight to thirteen days. There was one nuclear track above the filter in the first column that detected the alpha radiation of $^{214}Po$ emitted from the filter as above. The second column included the nuclear track detector above the mesh that detected the alpha radiation emitted by $^{214}Po$ of radon progeny that were unattached onto aerosols. The monitoring results are summarized in Table 4.

**Table 2**
Tracks counted on the same area of the Kodak LR-115, detector that was exposed to all sampled radon progeny on the filter (Column 1) and to attached radon progeny on the filter (Column 2). Sampling was carried out indoor.

| Indoor ground Level house | Tracks counted Column 1 No mesh | Tracks counted Column 2 Under mesh | Unattached fraction $f_p$ |
|---|---|---|---|
| Exposure No. 1 | 480 | 386 | 0.195 |
| Exposure No. 2 | 944 | 836 | 0.114 |
| Exposure No. 3 | 1322 | 1183 | 0.105 |

**Table 3**
Tracks counted on the same area of the Kodak LR-115, detector that was exposed to all sampled radon progeny on the filter (Column 1) and to attached radon progeny on the filter (Column 2). Sampling was carried out outdoor.

| Outdoor open cut uranium mine | Tracks counted Column 1 No mesh | Tracks counted Column 2 Under mesh | Unattached fraction $f_p$ |
|---|---|---|---|
| Exposure No. 1 | 899 | 810 | 0.100 |
| Exposure No. 2 | 878 | 810 | 0.077 |
| Exposure No. 3 | 1198 | 1081 | 0.098 |

**Table 4**
Tracks counted on the same area of the Kodak LR-115, detector that was exposed to all sampled radon progeny on the filter (Column 1) and to unattached radon progeny on the mesh (Column 2). Sampling was carried out indoor.

| Indoor ground level house | Tracks counted Column 1 No mesh | Tracks counted Column 2 Above mesh | Unattached fraction $f_p$ |
|---|---|---|---|
| Exposure No. 1 | 1263 | 114 | 0.090 |
| Exposure No. 2 | 1141 | 119 | 0.104 |
| Exposure No. 3 | 865 | 117 | 0.135 |

**Table 5**
The estimate of the lowest limit of detection.

| ST ST (h) | d.l.PAEC (μJ/m$^3$) |
|---|---|
| 24 | 0.3306 |
| 48 | 0.1653 |
| 72 | 0.1102 |
| 96 | 0.0826 |
| 120 | 0.0661 |

## 4. Discussion

### 4.1. Detection of $^{214}$Po by Kodak LR-115

The detector was calibrated by radon progeny inside the radon calibration chamber of the South Australian Environmental Protection Authority (Adelaide) and the Australian Radiation Protection and Nuclear Safety Agency, Melbourne. The potential alpha energy concentration (PAEC) of radon progeny was measured by the environmental radon progeny monitor during a second indoor (Table 2) and a third outdoor sampling period (Table 3). The average indoor and outdoor PAEC was measured as 0.0814 μJ m$^{-3}$ and 0.331 μJ m$^{-3}$ respectively and the sampled air volume was 2.257 m$^3$ and 2.160 m$^3$ respectively. These long-term average PAECs were also used with the tracks counted in Tables 2 and 3 to calibrate the detector:

The average potential alpha energy exposure of radon progeny to the $^{214}$Po track density [t (cm)$^{-2}$] conversion factor was calculated as 1.19E−4 μJ m$^{-3}$ V(m$^3$)/t (cm$^{-2}$).

It is feasible for example to scan 50 mm$^2$ of a nuclear track detector surface area and count 500 through tracks to maintain a relative standard deviation under 5%. Provided the flow rate is 0.25 L min$^{-1}$, the lowest PAEC of radon progeny that can be detected depends on the sampling time, ST (Table 5).

### 4.2. Error of the $f_p$ assessment

The error of $f_p$ that is estimated from results in Tables 2 and 3 takes into account:

(a) the statistical error of the detector alpha track count above the filter in the first column;

(b) the statistical error of the detector alpha track count in the second column;

(c) the error of the alpha track count difference in (a) and (b); and

(d) the error of the ratio of the alpha track count difference to the alpha track count of the detector in first column that had no mesh in (a).

**Table 6**
The relative error (%) of the "Unattached radon progeny fraction" ($f_p$) assessment from tracks counted on the same area of the Kodak LR-115, detector that was exposed to all sampled radon progeny on the filter and to unattached radon progeny on the mesh Table 4.

| Indoor ground level house | Unattached fraction $f_p$ | Error $f_p$ (%) 1$\sigma$ | Error $f_p$ (%) 2$\sigma$ | Error $f_p$ (%) 3$\sigma$ |
|---|---|---|---|---|
| Exposure No. 1 | 0.090 | 10 | 27 | 41 |
| Exposure No. 2 | 0.104 | 10 | 26 | 40 |
| Exposure No. 3 | 0.135 | 10 | 27 | 41 |

The error of $f_p$ that is assessed in Table 4 includes:

(a) the statistical error of the detector count above the filter in the first column;

(b) the statistical error of the detector alpha count above the mesh; and

(c) The error of the ratio of detector alpha counts in (a) and (b).

The error of the experimental results summarized in Table 4 is evidently the smallest one (the relative standard error has been presented in Table 6 for the 68%, 95% and 99% confidence level).

### 4.3. The penetration of −5 nm aerosols through the single mesh

The derivation of aerosol penetration through a wire mesh screen formed by uniform diameter fibers with circular cross section was first presented by [14]. If the particle diameter is below 1 μm, the particle deposition by gravitational settling and inertial impaction can be neglected. Here we need to separate the unattached fraction having less than 5 nm in diameter from the fraction attached to pre-existing aerosol being much larger. In that case we can also neglect particle deposition by interception, and are left with molecular diffusion as the dominant deposition mechanism. Assuming that the flow through the screens is laminar and Reynolds number is smaller than one, penetration of aerosol particles through a stack of screens can be described by a simplified relationship [15]:

$$P = exp(-2.7 B_f n Pe^{-2/3}) \tag{2}$$

where $P$ is penetration, $n$ is the number of screens in the stack, $P_e$ is the Peclet number defined as

$$P_e = \frac{U d_f}{D_p} \tag{3}$$

where $U$ is the velocity entering the screen, $d_f$ is the fiber diameter and $D_p$ is the diffusion coefficient of aerosol particle penetrating the screens. The term $B_f$ if defined by a relationship:

$$B_f = \frac{4\alpha h}{\pi(1-\alpha)d_f} \tag{4}$$

where $\alpha$ is the solid volume fraction of the screen, and $h$ is the thickness of the single screen. Diffusion coefficient was calculated from a Stokes–Einstein equation using the relationship:

$$D_p = \frac{kTC_c(d_p)}{3\pi\eta d_p} \tag{5}$$

where $k$ is the Boltzmann constant, $T$ is absolute temperature, $\eta$ is gas viscosity, $d_p$ is particle diameter and $C_c$ is the slip correction factor determined from an empirical relationship [16]:

$$C_c = 1 + 2\lambda/d_p(1.165 + 0.483 exp(-0.997 d_p/2\lambda)) \tag{6}$$

In the case of our particular screen type, fiber diameter $d_f$ = 30.48 μm, screen thickness h = 60.96 μm, solid volume fraction $\alpha$ = 0.366, duct internal diameter was 23 mm, nominal flow rate through the wire screen 0.25 L min$^{-1}$. At standard conditions 101.325 kPa and 20 °C, the penetration of 5 nm particles of unattached fraction through a single screen was determined by using Eq. (1) as less than 5% (see Fig. 2).

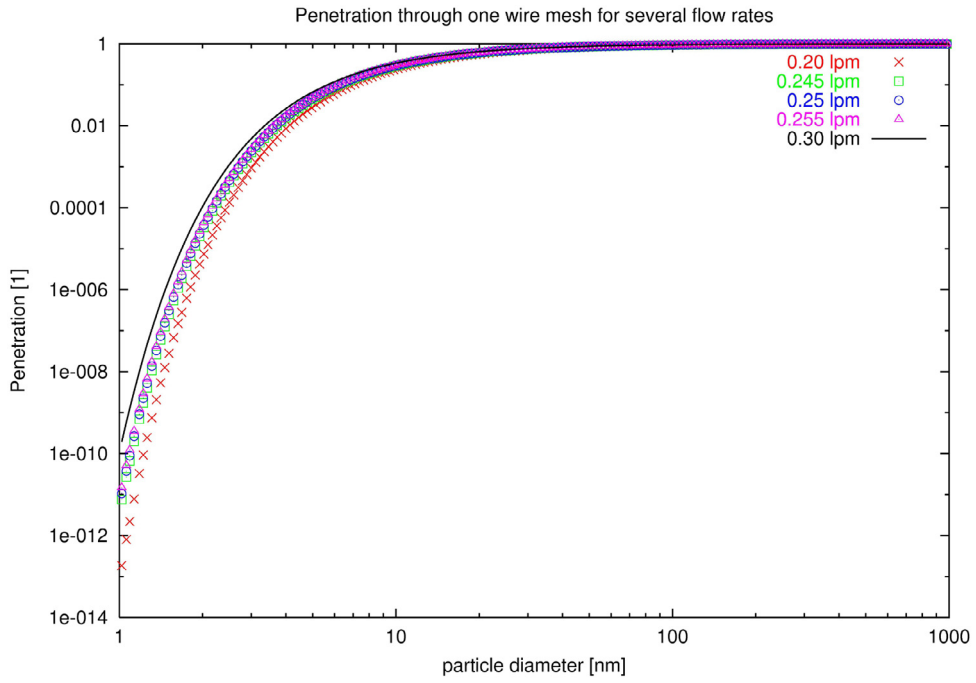


**Fig. 2.** Size-dependent penetration through a single wire screen for various flow rates.

## 5. Conclusion

Different nuclear track detector Kodak LR115, which detector's sensitive cellulose nitrate layer is stripped for etching and alpha tracks are counter by the spark-counter (detector I) was studied to estimate the thoron progeny unattached/attached concentration [17]. A similar experimental arrangement with the Kodak LR115 Type 2 was used to estimate the radon plus thoron progeny unattached/attached concentration through the optical counting of alpha tracks (detector II) [17]. The authors reported that the sensitivity factors for thoron and radon progeny unattached/attached concentration were approximately the same for the detector II with the Kodak LR115 Type 2 detector. As the radon progeny unattached/attached concentration is to be estimated from the 2 different detector readings the error of the measured radon progeny unattached/attached concentration could be high.

On the other hand the experimental arrangement of the detector Kodak LR-115 Type 2 that was outlined above detects only the alpha radiation of $^{214}$Po (radon progeny). Therefore, the proposed method is more suitable for the monitoring of the unattached/attached radon progeny concentration monitoring. The proposed unattached radon progeny fraction monitoring method that uses the nuclear track detector for the monitoring of the total radon progeny in air and the radon progeny above the single mesh has several advantages if compared with other methods:

(a) the long-term average unattached fraction of radon progeny is more appropriate for the personal dose assessment than the short-term unattached fraction;
(b) as the majority of unattached radon progeny below 5 nm is collected on the screen the proposed method measures the unattached radon progeny fraction with a high accuracy; and
(c) the proposed method is sensitive enough to be used for the occupational as well as the indoor monitoring of the unattached fraction of radon progeny.

It is equally important that the method is relatively inexpensive and therefore can be used on a wider scale than any other technique.

## CRediT authorship contribution statement

**Jiri Kvasnicka:** Outlined the concept of the method, Designed and constructed the "the unattached radon progeny fraction monitor", Carried out indoor monitoring, Optimized the response of the nuclear track detector to the alpha radiation of $^{214}$Po, Analysed the monitoring data, Drafted the paper manuscript, Edited the paper manuscript. **Vladimir Zdimal:** Developed the model for the assessment of the penetration of – 5 nm aerosols through the single mesh, Drafted the section 3.2, Edited the draft manuscript. **Allan Seini:** Selected a suitable monitoring site within the Ranger Uranium Mine stockpile area, Carried out the outdoor monitoring, Reviewed and edited the paper manuscript.

## Declaration of competing interest

The authors declare that they have no known competing financial interests or personal relationships that could have appeared to influence the work reported in this paper.

## References

[1] ICRP, The international commission on radiological protection 1990 recommendations of the international commission on radiological protection, in: ICRP Publication 60, Pergamon Press, 1990.
[2] Occupational intakes of radionuclides: Part 3, in: ICRP Publication 137, Ann, ICRP 46(3/4), ICRP, 2017.
[3] S.B. Solomon, M. Wilks, R.S. O'Brien, G. Ganakas, Particle Sizing of Airborne Radioactivity Field Measurements at Olympic Dam, Report ARL/TR113, Australian Radiation Laboratory, Yallambie, 1993.
[4] S.B. Solomon, R.S. O'Brien, M. Wilks, A.C. James, Application of the ICRP's new respiratory tract model to an underground uranium mine, Radiat. Prot. Dosim. 53 (1994) 119–125.
[5] J. Porstendorfer, Radon: measurements related to dose, Environ. Int. 22 (1) (1996) S563–S583.
[6] Y.-S. Cheng, T.-R. Chen, P.T. Wasiolek, A. Van Engen, Radon and radon progeny in the carlsbad caverns, Aerosol Sci. Technol. 26 (1997) 74–92.
[7] A. Reineking, J. Porstendorfer, 'Unattached' fraction of short-lived Rn decay products in indoor and outdoor environments: an improved single-screen method and results, Health Phys. 58 (1990) 715–727.
[8] A. Vargas, X. Ortega, M. Porta, Dose conversion factor for radon concentration in indoor environments using a new equation for the F–fp correlation, Health Phys. 78 (2000) 80–85.

[9] Q. Guo, L. Zhang, L. Guo, Assessment of the unattached fraction of indoor radon progeny and its contribution to dose: a pilot study in China, J. Radiol. Prot. 32 (2012) 447–454.
[10] J. Kvasnicka, Radon concentration in the soil air measured by track detectors, Nucl. Instrum. Methods 174 (1980) 599.
[11] J. Kvasnicka, Radon concentration in water measured by track detectors, Nucl. Instrum. Methods 206 (1983) 563.
[12] J. Kvasnicka, J. Cabanek, Detection sensitivity of track detector KODAK LR-115 to alpha particle energy and irradiation angle, Czech. J. Phys. B 32 (1982) 355.
[13] J. Kvasnicka, Theory of alpha activity measurement by nuclear track detectors, Nucl. Tracks Radiat. Meas. 11 (1–2) (1986) 81–84.
[14] Y.S. Cheng, H.C. Yeh, Theory of a screen type diffusion battery, J. Aerosol Sci. 11 (3) (1980) 313–320.
[15] Y.S. Cheng, Y.F. Su, G.J. Newton, H.C. Yeh, Use of a graded diffusion battery in measuring the radon activity size distribution, J. Aerosol Sci. 23 (1992) 361–372.
[16] J.H. Kim, G.W. Mulholland, S.R. Kukuck, D.Y.H. Pui, Slip correction measurements of certified PSL nanoparticles using a nanometer differential mobility analyzer (nano-DMA) for Knudsen number from 0.5 to 83, J. Res. Natl. Inst. Stand. Technol. 110 (1) (2005) 31–54, https://www.ncbi.nlm.nih.gov/pmc/articles/PMC4849562/.
[17] R. Mishra, B.K. Sapra, Y.S. Mayya, Development of and integrated sampler based on direct 222Rn/220Rn progeny sensors in flow-mode for estimating unattached/attached progeny concentration, Nucl. Instrum. Methods Phys. Res. B 267 (2009) 3574–3579.